Available online at www.sciencedirect.com

ScienceDirect

Procedia CIRP 111 (2022) 496–500

www.elsevier.com/locate/procedia

12th CIRP Conference on Photonic Technologies [LANE 2022], 4-8 September 2022, Fürth, Germany

Macroscopic simulation model for laser cutting of carbon fibre reinforced plastics

Jan Keuntje[a]*, Selim Mrzljak[b], Lars Gerdes[b], Verena Wippo[a], Stefan Kaierle[a,c], Ludger Overmeyer[a,c], Frank Walther[b], Peter Jaeschke[a]

[a]*Laser Zentrum Hannover e.V., Hollerithallee 8, 30419 Hannover, Germany*
[b]*TU Dortmund University, Chair of Materials Test Engineering (WPT), Baroper Str. 303, 44227 Dortmund, Germany*
[c]*Leibniz University Hannover, Institute of Transport and Automation Technology, An der Universität 2, 30823 Garbsen, Germany*

*Corresponding author. *E-mail address:* j.keuntje@lzh.de

Abstract

Laser cutting of carbon fibre reinforced plastics (CFRP) has shown promising potential as an alternative to conventional manufacturing processes. Laser cutting has major benefits of contactless and therefore wear-free machining and high automation potential. The main challenge is to reduce the heat input into the material during the process. Excessive temperatures cause damage within the surrounding matrix material and could locally modify the structural properties of the CFRP. For industrial use it is necessary to be able to predict the resulting temperature fields. To gain knowledge of the temperature distribution during the process, a three-dimensional macroscopic finite element model is developed using ANSYS simulation software. Transient-thermal analyses are performed and the material removal process is implemented via the element-death technique. Simulations are run for a unidirectional composite structure and different cutting speeds. The resulting temperatures are compared to experimental data.

Keywords: laser cutting simulation ; carbon fibre reinforced plastics ; heat affected zone ; finite element method

1. Introduction

The demand for CFRP applications is increasing continuously, focussing primarily on lightweight design and energy efficiency in the aerospace or automotive industries [1]. CFRP stand out due to their excellent strength-to-weight ratio, high damage tolerance and good corrosion resistance. But the machining of CFRP involves some challenges. The production is mainly performed by conventional machining techniques, like milling or waterjet cutting. Although these techniques are well established, they still have drawbacks such as high tool wear, insufficient quality, complex setup and hence limited flexibility [2]. Laser cutting offers the benefit of potentially cutting fully automated with a constant quality at high feed rates while also operating wear-free [3]. Nevertheless, the heat generated during the laser cutting process can damage the bulk material and lead to a heat affected zone (HAZ) around the cut faces. These areas influence the mechanical properties. The expansion of the HAZ depends on the fibre orientation and the processing parameters. Heat is mainly conducted along the fibres causing further damage in surrounding matrix material, which sublimation temperature is much lower compared to that of carbon fibres. The propagation of the HAZ into the adjacent material is the main criterion to evaluate the process quality [4,5].

The experimental investigation of the HAZ can either be done using microscopic analysis and digital imaging, but also by detecting temperatures during the process, e.g. using thermography. To gain knowledge about the expansion of the HAZ beforehand, numerical simulations should be performed.

10.1016/j.procir.2022.08.078

The modelling of laser machining is mainly focused on metallic alloys [6]. Regarding composites, three-dimensional simulations via finite element method (FEM) often deal with models on a microscopic scale. Hence, model sizes are limited to the magnitude of hundreds of micrometres, whether a heterogeneous fibre-matrix mesh [7,8] or a homogenized material model [9] is used.

For analysing the formation of the HAZ and the ablation mechanisms, a heterogeneous approach – separating between fibre and resin – with a microscopic resolution is well suited. For process design and the observation of temperature fields during laser machining of real structures, a simulation of a higher magnitude is necessary. Heterogonous models with such a fine mesh aren't practical for these schemes, due to high computation times. Therefore, this work aims to present an approach, focussing on a macroscopic scale, targeting to predict the evolution of the temperature field. In this context, this study will introduce a transient-thermal model and compares simulation results to experimental data, obtained by thermal imaging of the laser cutting process.

2. Experimental setup

The experiments were conducted with a thin-disk high power nanosecond laser TruMicro 7050 from the TRUMPF Laser GmbH, emitting at a wavelength of 1030 nm. The laser delivers a tophat intensity distribution with a spot diameter of 1.2 mm. All laser parameters are summarised in Table 1. To protect the focusing optics, a gas flow is applied by a ring jet, which simultaneously has a cooling effect on the material. The setup is schematically presented in Fig. 1.

The CFRP material consists of six layers of unidirectional carbon fibre tape and an epoxy resin with a fibre volume fraction of 59.2 %. The material is supplied by the ERC GmbH. The relevant properties are listed in Table 2, which are provided by the supplier and are complemented through literature values.

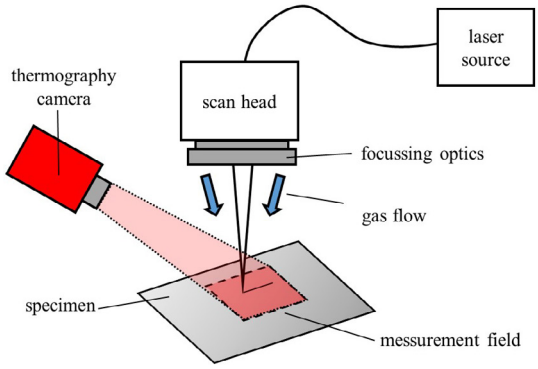

Fig. 1. Experimental setup

The cutting velocity (v_{cut}) was used as an experimental factor. A repetition rate of 18.8 kHz was chosen. At this rate, the maximum average output power of 1.5 kW, as well as the maximum pulse energy of 80 mJ, can be used. The cutting length was set to 20 mm and the investigated cutting direction was parallel to the fibres. To obtain a full cut through the material a multipass cutting strategy has to be applied consisting of several laser beam passes over the workpiece. In the scope of this work, only a single pass is analysed.

The surface temperature is detected with the ImageIR® 8300 thermography camera (TC) from Infratec GmbH. The camera provides a measurement field of 38 × 48 mm², a pixel size of 75 µm and was positioned at a distance of 0.51 m at an angle of 40° relative to the specimen surface. A measurement frequency at a quarter frame window of 800 Hz was used.

Table 1. TruMicro 7050 laser specifications

Laser parameter	Value
Max. avg. laser power, $P\ (W)$	1500
Wavelength, $\lambda\ (nm)$	1030
Pulse duration, $t_p\ (ns)$	30
Maximum pulse energy, $E_p\ (mJ)$	80
Repetition rate, $f\ (kHz)$	5 - 50
Spot diameter, $d_s\ (mm)$	1.2

Table 2. Simulation material parameters, (a) supplier (b) literature [10,11]

Material property	Carbon fibre	Epoxy resin	Laminate
Density, $\rho\ (kg/m^3)$	1780[a]	1280[a]	1575
Specific heat capacity, c $\left(J/_{kg*K}\right)$	875[a]	1200[a]	982.7
Thermal conductivity, k $\left(W/_{m*K}\right)$	$\parallel$ 50[b] $\perp$ 5[b]	0.2[a]	$\parallel$ 31.64 $\perp$ 0.68
Thermal diffusivity, α $\left(m^2/_s\right)$	$\parallel$ 3.21 e^{-5} $\perp$ 3.21 e^{-6}	1.3 e^{-7}	$\parallel$ 2.04 e^{-5} $\perp$ 4.39 e^{-7}
Evaporation temperature, $T_s\ (°C)$	3650[b]	500[b]	–

3. Finite element model

The purpose of the model is to calculate the temperature distributions and material removal due to the energy input entered by laser radiation.

A three-dimensional solid model is developed with temperature as the only degree of freedom applied. The generated mesh is homogenised according to the fibre volume fraction. It is not necessary to consider different material orientations because a unidirectional laminate is used. The relevant composite properties are calculated via the rule of mixture. This procedure is permitted, because the global temperature expansion is to be investigated. As shown in Table 2, the difference between thermal conductivity parallel and perpendicular to the fibre direction is significant, which generates a strong anisotropic behaviour.

The size of the model is set to 100 × 25 mm². These dimensions ensure that enough material around the actual cut is modelled. Hence heat can conduct into the bulk material. Within the cutting area a structured, fine resolved mesh is used with an element size of 10 µm in through thickness direction. Elsewhere a free mesh is generated. Due to symmetry, only a half model is created, as shown in Fig. 2. In total 317,984 elements are generated.

The ablation depth per pulse depends on the optical and thermal penetration depth of the material. For CFRP and a timespan of a few nanoseconds, this length is less than a micrometre. If a single pass would be modelled by simulating every single pulse, the element size in through thickness

direction had to be chosen according to this length. Attempting this would result in a microscopic approach requiring a heterogeneous mesh. Additionally, a cutting length of 2 mm, a repetition rate of 18.8 kHz and a cutting speed of e.g. 3 m/s would yield in a number of 125 pulses per pass. Lower velocities would even further increase the number of pulses. In combination with a microscopic mesh, this would lead to a high amount of computational effort and is therefore not practical.

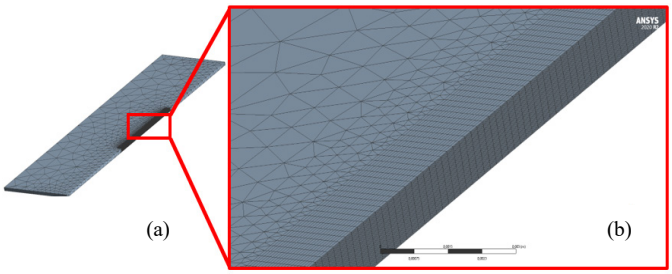

Fig. 2. (a) View of the half-model, (b) dense mesh within the cutting area

As an initial approach, the laser cut is estimated as a line source, which is especially true for high cutting velocities. Furthermore, the following assumptions were made:

- The material properties are uniformly homogenised after the fibre volume fraction.
- Pores or any defects in the material are neglected.
- Thermophysical material properties are constant.
- The laser beam distribution is uniform and ideal.
- Vaporisations or phase change effects are neglected.
- Sublimated material is completely removed.
- Bulk and surrounding air temperature is set to 18 °C.
- Radiation heat losses are neglected.

The heat input by the laser is implemented as a heat flux. To calculate the input power, the energy of all pulses within one pass is accumulated and divided by the cutting time. The chosen repetition rate of 18.8 kHz yields the maximum average output power available.

The input power is spread uniformly over the whole cutting area, which is simplified represented by the cutting length and the spot diameter. Additionally, an absorption coefficient of 0.9 is added according to [12]. The time for the heat load step is known through the cutting length and velocity. Afterwards, the heat flux is set to zero, representing the cooling phase without laser material interaction. Around the surrounding surfaces, free convection to the atmosphere is applied. Due to the gas jet, the convection on the top surface has to be considered as forced convection. The convection coefficient is approximated regarding the flow conditions. For simplification, the relations for forced convection to a vertical plane are assumed [13]. The material removal is executed at the end of the heat load step. All element temperatures are checked. If they exceed the sublimation temperature of 3650 °C, they are deactivated from the model.

4. Results

First simulation results using the estimation of a line energy source showed that the remaining temperatures exceeded the experimental observations by far. This can be explained by the real interaction time between the laser and the material. In the model, the sublimation temperature is rapidly reached during the heat load step. But all affected elements are foremost deleted after the full cut is completed. So, elements, which temperatures exceed the sublimation temperature, still conduct heat into the surrounding material. While in reality, the interaction time is in the range of nanoseconds and therefore the conduction is much lower in this time-span than in the simulation.

To increase the accuracy of the model, the cutting process is separated into equal time steps. This way the progressive character of a cut is generated. The heat flux for every step is adopted according to the corresponding length travelled per step. This way, elements, which are sublimated at the beginning of the cut, do not conduct further energy to adjacent elements while the cut is still in progress. Further tests have shown, that with an increasing number of steps, the remaining temperature decreases as expected. At a number of 25 time steps, the decline in temperature is getting small and the additional computation time is still acceptable.

The measured temperatures are compared to the simulation results. For evaluation purposes, a time period of one second after completion of a cutting pass is covered. The time point zero is specified as the beginning of the cooling phase. This point is clearly defined within the simulation. But, for the experiments, this point cannot be exactly determined because of the measuring frequency of the TC. Therefore, the first frame with a recognisable temperature deflection is set as the beginning of the pass. Then the known cutting time is added. The nearest frame after this time is chosen as the beginning of the cooling phase. In doing so, a maximum error of 1.25 ms $(1/f)$ has to be considered.

Another error to deal with is the exact emission coefficient of CFRP, which is unknown. Based on preliminary experiments an emission coefficient of $\varepsilon = 0.92$ is estimated. Deviations are considered by applying a delta of $\Delta\varepsilon = \pm 0.03$. This leads to a maximum temperature difference of less than 2.5 °C for the highest measured temperatures.

In Fig. 3 the thermographic image for a cutting velocity of 3 m/s at 50 ms after the start of the cooling phase is shown. The scale ranges from 18 °C (dark blue) to 80 °C (pink). Measurement points are chosen at six different lines across the cutting kerf. For every spot of interest, the mean value out of the six lines is calculated. To ensure that the distances on all six lines are comparable, the centre of the kerf has to be determined. This is done by identifying positions with the same temperature on each side of the kerf. The half distance of these points is set as the midpoint. This procedure is executed 50 ms into the cooling phase and for a temperature of 50 °C. To compare experimental and simulation results it is stated, that the distance to the middle and not the edges of a pixel is taken as comparative value. Because the mesh resolution is different from the pixel array, linear interpolation within the simulation results is done, if it is necessary to meet the same distances.

The left graph of Fig. 3 shows the maximum standard deviation (SD) over the entire cooling phase for a cutting speed of 3 m/s, exemplary for this investigation. There is a peak right at the beginning of the cooling phase. These high deflections can be explained by emissions influencing the measurement.

At time points near the end of the actual cut, reflections of a hot plume and hot ablation products are recorded within the measurement field. This leads to some noise in the temperature data. After 50 ms the maximum SD stays lower than 2 °C and after 300 ms it is lower than 0.5 °C.

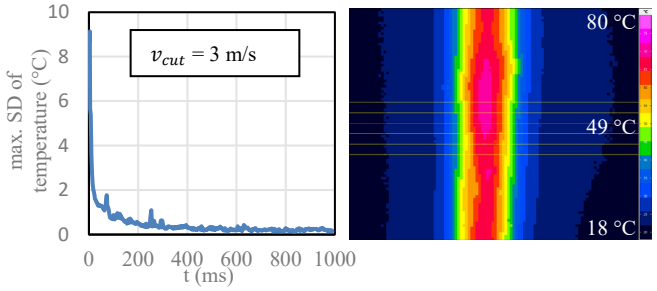

Fig. 3. The maximum standard deviation of the temperature (left), lines of measurement in a thermographic image, t = 50 ms (right)

Fig. 4 shows the comparison between the measured and simulated temperatures at different distances (s) from the cutting edge.

Two different cutting speeds are considered. A slower cutting speed equals longer interaction time and therefore an increased energy input and residual heat. This can be seen from both the measured (dashed lines) and the simulated (symbols) data. The maximum recorded temperatures are limited through the calibration range of the TC, which is around 90 °C in this setup. This limit value is reached during the cut and still occurs at time zero, after which the temperature drops exponential. This corresponds to a typical temperature progression through heat conduction. Heat flows from its source into the material. The larger the difference to the bulk temperature, the faster the heat conducts. The temperature progression is also affected by convection.

At 75 µm and 150 µm distance from the kerf, the simulation results fit well to this measured data over the entire cooling phase. The largest differences of about 3.8 °C to 5.8 °C occur within the first 50 ms to 100 ms. It has to be mentioned that this is the timespan with the highest SD. Afterwards, the gaps drop and stay mostly below 2 °C. At a larger distance (s = 225 µm), deviations between simulation and measured values are higher. The measured data still follows the characteristics described above. However, in the simulation, the maximum temperatures are not present at time zero. Instead, there is a brief rise in temperature in the beginning due to heat conduction, followed by the typical decline. From about 200 ms on, the two curves are again close to each other.

This difference can be explained by the assumptions made in the model, neglecting all kinds of vaporisation effects. As mentioned before, the start of the cooling phase is heavily influenced by process emissions, which are present over the whole recorded vision field. Further away from the kerf, the hot plume seems to have a relevant influence on the surface temperature within the first 100 to 200 ms. The model, in contrast to reality, only considers heat, which is conducted away from the kerf. Besides this, the following factors influencing the results have to be accounted for:

- The experimental setup doesn't allow an ideal measurement angle for the TC.
- The real emission coefficient changes with surface temperature.
- Measured temperatures are depending on pixel size and position.

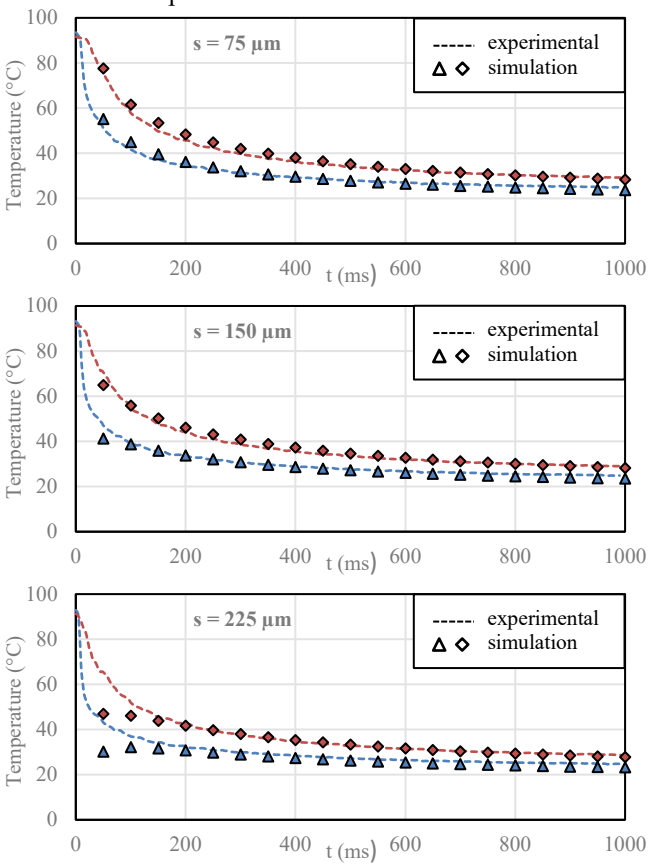

Fig. 4. Comparison between measured and simulated temperature progression at increasing distances s from the kerf; v_{cut} = 3 m/s (blue), v_{cut} = 1 m/s (red)

5. Conclusion and outlook

In this work, a macroscopic simulation model was developed to predict the temperature field expansion during the laser cutting process of CFRP. Simulation results are in good agreement with the measured data, at least within 150 µm of the cutting edge. At 225 µm the consistency of data is given from about 200 ms on into the cooling phase. It might be probable, that differences further increase with lower cutting speeds. These limitations have to be considered, describing the validity of the model. The discrepancies can be explained by the occurring vaporisation effects that additionally heat the material surface, but are not considered in this model. This seems to be the most relevant simplification made in the setup of the model and should be investigated in future studies. Nevertheless, the conductive behaviour is well demonstrated by the approach presented in this work.

The next step of research is the simulation of the heat accumulation caused by multiple laser beam repetitions. In addition, there is a lot of room for further investigations, considering more experimental factors, like the repetition rate, the laser power or the cutting direction.

Another aspect to look at is the usage of further temperature measurement methods, e.g. thermocouples. These could be embedded in the material and used to detect internal temperatures as a supplement to the surface temperature measurement.

Acknowledgements

The authors gratefully acknowledge the funding by the German Research Foundation (Deutsche Forschungsgemeinschaft, DFG) of the project “Characterization and modelling of the laser based separation process and resulting damage mechanisms of carbon fibre-reinforced plastics under fatigue loading” (project number 436398518).

The authors would also like to thank the TRUMPF Laser GmbH for providing the TruMicro 7050 laser source.

References

[1] Sauer, M. Composites Market Report 2020 - The Global CF-Market 2020 -. Composites United e.V., Germany, 2020.

[2] Karataş, M. A., and Gökkaya, H. A Review on Machinability of Carbon Fiber Reinforced Polymer (CFRP) and Glass Fiber Reinforced Polymer (GFRP) Composite Materials. Defence Technology, Vol. 14, No. 4, 2018, pp. 318–326.

[3] Steen, W. M., and Mazumder, J. Laser Cutting, Drilling and Piercing. In Laser Material Processing, Springer, London, 2010, pp. 131–198.

[4] Herzog, D., Jaeschke, P., Meier, O., and Haferkamp, H. Investigations on the Thermal Effect Caused by Laser Cutting with Respect to Static Strength of CFRP. International Journal of Machine Tools and Manufacture, Vol. 48, Nos. 12–13, 2008, pp. 1464–1473.

[5] Bluemel, S., Jaeschke, P., Wippo, V., Bastick, S., Stute, U., Kracht, D., and Haferkamp, H. Laser Machining of CFRP Using a High Power Fiber Laser – Investigations on the Heat Affected Zone. Proceedings of the 15th European Conference on Composite Materials, 2012.

[6] Parandoush, P., and Hossain, A. A Review of Modeling and Simulation of Laser Beam Machining. International Journal of Machine Tools and Manufacture, Vol. 85, 2014, pp. 135–145.

[7] Negarestani, R., Sundar, M., Sheikh, M. A., Mativenga, P., Li, L., Li, Z. L., Chu, P. L., Khin, C. C., Zheng, H. Y., and Lim, G. C. Numerical Simulation of Laser Machining of Carbon-Fibre-Reinforced Composites. Proceedings of the Institution of Mechanical Engineers, Part B: Journal of Engineering Manufacture, Vol. 224, No. 7, 2010, pp. 1017–1027.

[8] Yang, H., Liu, H., Gao, R., Liu, X., Yu, X., Song, F., and Liu, L. Numerical Simulation of Paint Stripping on CFRP by Pulsed Laser. Optics & Laser Technology, Vol. 145, 2022, p. 107450.

[9] Zhang, J. F., and Long, L. C. Finite Element Simulation for Laser Ablation of Carbon Fiber Epoxy Composite. Applied Mechanics and Materials, Vols. 66–68, 2011, pp. 715–720.

[10] Sheng, P., and Chryssolouris, G. Theoretical Model of Laser Grooving for Composite Materials. Journal of Composite Materials, Vol. 29, No. 1, 1995, pp. 96–112.

[11] Freitag, C. Energietransportmechanismen bei der gepulsten Laserbearbeitung Carbonfaser verstärkter Kunststoffe (Dissertation). Herbert Utz Verlag, Wissenschaft, München, 2017.

[12] Freitag, C., Alter, L., Weber, R., and Graf, T. Theoretical and Experimental Determination of the Polarization Dependent Absorptance of Laser Radiation in Carbon Fibers and CFRP. Lasers in Manufacturing 2015.

[13] Merker, G. P. Wärmeübergang Bei Der Umströmung Zylindrischer Körper. In Konvektive Wärmeübertragung, Springer Berlin Heidelberg, Berlin, Heidelberg, 1987, pp. 223–269.